Reactivity and Photoionization Studies of Bimetallic Cobalt−Manganese Clusters

G. M. Koretsky, K. P. Kerns, G. C. Nieman,† M. B. Knickelbein,* and S. J. Riley*

Chemistry Division, Argonne National Laboratory, Argonne, Illinois 60439

Received: November 12, 1998; In Final Form: February 1, 1999

The reactivity of selected Co_nMn_m ($8 \leq m + n \leq 23$) clusters with N_2 and the vertical ionization potentials (IPs) of selected Co_nMn_m ($8 \leq m + n \leq 31$) clusters have been measured. No obvious correlation is found between the reactivities and the IPs. Inferences about cluster structure may be made from the nitrogen uptake data. In particular, whereas pure cobalt clusters tend to adopt structures having bulk packing, incorporation of manganese atoms into the cluster shifts the relative energies of close-lying isomers to favor an icosahedral growth sequence. For many cluster sizes, the maximum number of nitrogen molecules adsorbed on a cluster at −80 °C is equal to the number of cobalt atoms on the surface of the cluster, thereby giving insight into the cluster structure and the locations of the individual cobalt and manganese atoms in these bimetallic species.

1. Introduction

The physical and chemical properties of bimetallic particles are of great interest in the field of catalysis because the activity and selectivity toward industrially important reactions on bimetallic surfaces often differ greatly from those observed on surfaces of the component metals. Bimetallic systems have been investigated thoroughly by the surface science community in recent years.[1] Simultaneously, the field of cluster science has grown rapidly, stimulated in large part by the development of the laser vaporization technique,[2] which provides a general method for producing small clusters of metals, semiconductors, and other materials. While the vast majority of experimental cluster research has focused on the structural, electronic, and chemical properties of homonuclear clusters, several studies of heteronuclear clusters of transition metal elements, main group metal elements, semiconductor elements, or some combination thereof have been performed. In particular, the abundance distributions of Ni_nCr_m and Ni_nAl_m were examined to explain the growth patterns of these clusters,[3] and photodissociation was applied to Bi_nFe_m,[4] Bi_nCr_m,[4] and Fe_nAg_m[5] to investigate the intermetallic bonding. Also, among the notable developments, the reactivities of Co_nAl_m[6] and Co_nV_m[7] with H_2 were probed, and the ionization potentials of Co_nAl_m[8,9] and Co_nV_m[10] were measured to provide information on the electronic structure.

Other than an early report of the generation of Co_nMn_m clusters,[11] the cobalt−manganese system has not been as extensively studied as many other bimetallic combinations. Co−Mn particles have been produced by the process of solvated metal atom dispersion (SMAD), and their catalytic properties have been investigated.[12] For 1-butene hydrogenation and isomerization as well as 1,3-butadiene hydrogenation, it has been found that small amounts of Mn greatly increase the activity of a Co/SiO_2 SMAD catalyst. Despite this interesting observation, the chemical and physical properties of Co_nMn_m clusters have not been studied in detail to date. In this paper, we report the vertical ionization potentials (IPs) of selected Co_nMn_m ($8 \leq m + n \leq 31$) clusters and the reactivity of selected Co_nMn_m ($8 \leq m + n \leq 23$) clusters with N_2.

In the reactivity studies, nitrogen is used as a probe of cluster structure by a determination of the uptake of nitrogen, i.e., the extent of cluster coverage, as a function of N_2 pressure. The interpretation of such chemical probe data to provide structural information depends on how the probe species binds to the cluster under investigation. Dinitrogen adsorbs nondissociatively on both cobalt and manganese surfaces.[13] A previous study of the uptake of N_2 on cobalt clusters was likewise interpreted in terms of nondissociative adsorption.[14] This is in contrast to an earlier study of the reactions of cobalt clusters at 50 °C, in which the reactivity pattern of Co_n with N_2 was found to be quite similar to that of dissociatively chemisorbed D_2 and unlike that of molecularly chemisorbed CO.[15] This was interpreted as indicating the adsorption of N_2 on Co_n is dissociative. However, it seems more likely that the reactivity is governed by an initial physisorption step for both N_2 and D_2,[16] and nitrogen dissociation need not be invoked to explain the similar kinetics. In the present experiments, we find that the amount of nitrogen adsorbed on Co_nMn_m decreases with increasing temperature, consistent with a nondissociative exothermic adsorption reaction at equilibrium. Furthermore, we find little change in the ionization potentials of Co_nMn_m upon adsorption of N_2, which is also consistent with molecular adsorption. If dissociative chemisorption was occurring, entirely new species, metal nitrides, would be made that most likely would have substantially higher IPs and would be the products of nonequilibrium reactions. We thus assume that in the present case nitrogen adsorption is nondissociative. This is in contrast to the adsorption of N_2 on molybdenum and tungsten surfaces[13] and clusters of these metals,[17,18] where it was inferred that dissociation into atomic nitrogen does take place.

2. Experimental Methods

The experimental apparatus and methods used to record photoionization efficiency (PIE) spectra for the determination of IPs have been described in detail previously.[19] To summarize, metal atoms are generated by focusing the output of a pulsed Nd:YAG laser onto the surface of a 0.64 cm diameter target rod of composition $Co_{0.85}Mn_{0.15}$. Cluster growth and cooling occur in helium carrier gas flowing within a 7.6 cm × 0.32 cm (length × i.d.) flow tube maintained near 70 K and at a pressure

† Permanent address: Chemistry Department, Monmouth College, Monmouth, IL 61462.

10.1021/jp9844157 CCC: $18.00
Published on Web 03/12/1999

of approximately 15 Torr. The clusters reside about 1.0 ms in the flow tube before undergoing a mild supersonic expansion through a 1.3 mm diameter orifice. Thereafter, they travel into a differential pumping region and into a detection chamber held at 10^{-6} Torr. Once inside the detection chamber, the molecular beam passes between the ion extraction grids of a time-of-flight (TOF) mass spectrometer, where it is intersected at 90° by tunable ultraviolet light, produced by frequency-doubling the output of a pulsed dye laser (~15 ns pulse length) and timed to reach the clusters as they pass within the ion extraction region. Laser fluences are attenuated to ≤ 200 μJ cm^{-2} so that one-photon photoionization events far exceed two-photon photoionization and fragmentation events. A microchannel plate ion detector is used to detect the mass-separated cluster ions. After a total of 2000 TOF spectra at a given laser wavelength are digitized and added using a digital oscilloscope, the summed spectrum is transferred to a microcomputer for analysis and the laser is tuned to the next wavelength.

To correct for random fluctuations in the cluster intensity, a normalization procedure is employed as part of the process for obtaining PIE spectra.[20] Two TOF spectra are alternately recorded, one in which photoionization is accomplished using the frequency-doubled dye laser and a second reference TOF spectrum measured using an ArF (193 nm) laser. The integrated mass peak areas from the former spectrum are then divided by the integrated mass peak areas from the latter spectrum to give the doubly normalized relative ionization cross section $\sigma(\lambda)$:

$$\sigma(\lambda) = [I_\lambda/F_\lambda]/[I_{193}/F_{193}] \quad (1)$$

where I and F are the TOF peak areas and laser fluences, respectively.

The experimental apparatus and methods used to measure the uptake of N_2 on Co_nMn_m are similar to those used for the IP determinations, and they have also been described in detail previously.[21] Briefly, in the flow tube downstream from where cluster growth terminates, nitrogen gas is added either as pure N_2 or as a mixture in helium. A typical reaction time for the flows used is ~0.8 ms. Following expansion out of a nozzle, the cluster beam passes through a differential pumping stage to reach a detection chamber, where the clusters are ionized by the fixed-frequency light from either an ArF laser (6.42 eV photon energy) or an F_2 laser (7.89 eV photon energy). The mass analysis is via a reflectron TOF mass spectrometer. In this apparatus, the temperature of the cluster source and flow tube could be varied from −160 to 150 °C. To study the reactivity over a broader range of cluster compositions, two bimetallic rods were used in these experiments: the $Co_{0.85}Mn_{0.15}$ rod and a rod of composition $Co_{0.5}Mn_{0.5}$.

In general, the ArF laser was used to ionize both the bare Co_nMn_m clusters and the products of their reaction with N_2. However, some of the smaller clusters ($n + m \leq 5$) could not be ionized by the lower-energy photons from the ArF laser. For these, the F_2 laser was used.

3. Results

Representative TOF spectra of the bimetallic clusters are shown in Figure 1. Panels a and b show the distributions produced from the $Co_{0.85}Mn_{0.15}$ and $Co_{0.5}Mn_{0.5}$ targets, respectively. The cluster distributions are close to what would be expected on purely statistical grounds,[3] assuming that the composition of metal vapor is identical to that of the target, although there is a slight enrichment in cobalt (i.e., the weighted percentage of cobalt in all of the clusters in panel a is slightly higher than 85% and in panel b is slightly higher than 50%). This enrichment is most pronounced for the smaller clusters, paralleling previous observations of bimetallic cluster abundance distributions.[3] Also, there is no minimum number of cobalt or manganese atoms required to produce stable clusters, contrary to the observations reported earlier by Sone et al.,[11] who claim that Co_nMn_m clusters can be efficiently produced only when $n \geq 4$, suggesting that a core of Co_4 is necessary for producing these species. We observe clusters in which $n < 4$ and see no sudden increase in cluster abundance at $n = 4$.

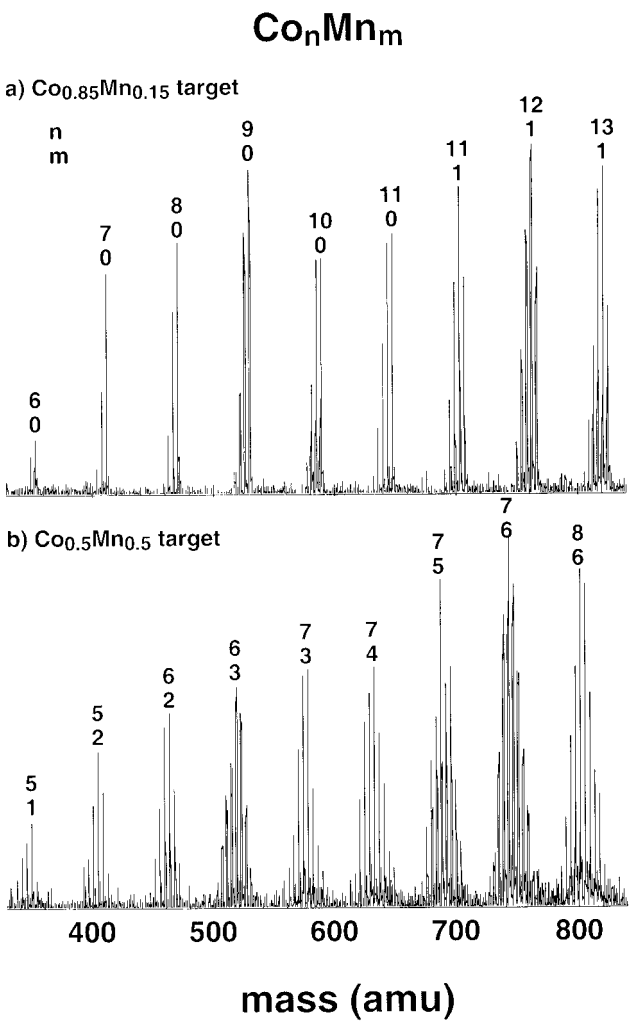

Figure 1. Time-of-flight mass spectra of Co_nMn_m, ionized by the ArF laser ($h\nu = 6.42$ eV). For each cluster size, the most abundant peak is labeled according to ^n_m. The distributions produced from the $Co_{0.85}Mn_{0.15}$ and $Co_{0.5}Mn_{0.5}$ rods are shown in panels a and b, respectively.

Representative PIE spectra are shown in Figures 2−4. In general, the photoionization cross sections increase monotonically with increasing photon energy above threshold, consistent with high densities of low-lying vibronic states in the cluster ions.[22,23] Vertical IPs were obtained from the PIE spectra by linearly extrapolating the major post-threshold portion of the PIE curve to the signal baseline, as discussed in ref 19. The IPs for Co_nMn_m ($8 \leq m + n \leq 31$) determined from this procedure are shown in Figure 5 and listed in Table 1. The ±0.05 eV error limits reflect the uncertainty in the extrapolation procedure.

In Figures 6−8, we show nitrogen uptake plots for Co_nMn_m produced from the $Co_{0.85}Mn_{0.15}$ rod for $n + m = 8-20$ at −80 °C. In these plots, the average number of N_2 molecules $\bar{p}$ adsorbed on the cluster is plotted against the N_2 pressure, the latter on a logarithmic scale. $\bar{p}$ is calculated from the distribution

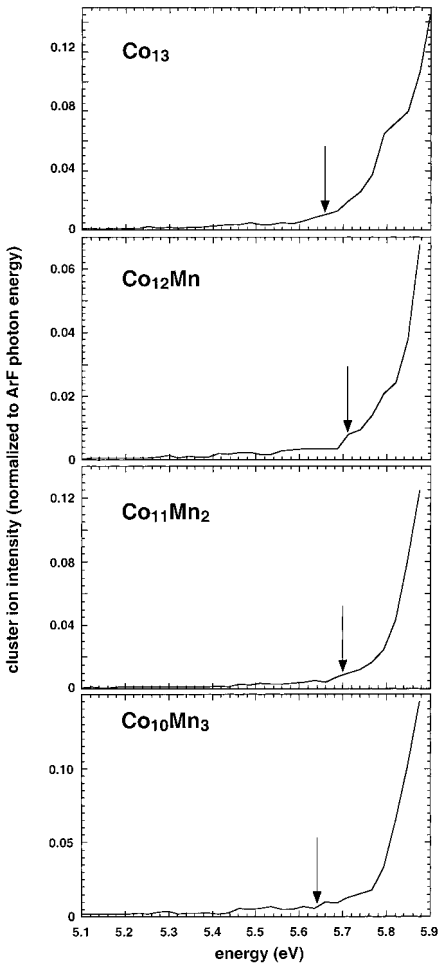

Figure 2. Photoionization efficiency spectra of Co_nMn_m, $n + m = 13$. The assigned vertical IPs are indicated with arrows.

of $Co_nMn_m(N_2)_p^+$ peaks in the mass spectra. For many of the clusters, at some N_2 pressures there are two groups of $Co_nMn_m(N_2)_p^+$ peaks. Such bimodal distributions are most likely due to the presence of more than one isomer of Co_nMn_m. When the two groups of peaks are sufficiently well separated in the mass spectra, independent values of $\bar{p}$ are calculated and plotted in Figures 6−8. When they are not, data points are averages over the whole distributions and are labeled with B.D. in Figures 6 and 7.

For a given cluster size (i.e., a given value of $n + m$), it is readily seen that both the maximum number of nitrogen molecules adsorbed and the initial reactivity in the limit of zero coverage depend on the stoichiometry of the bimetallic cluster. For example, Co_{13} eventually saturates with an uptake of 12 N_2 molecules, which is greater than the N_2 saturation level for the bimetallic 13-mers. At the lowest nitrogen pressures, however, $\bar{p}$ is lower for Co_{13} than for its bimetallic counterparts. A closer inspection of the mass spectra at −40 °C reveals that all of the 13-mers appear to have more than one isomer, as evidenced by bimodal p distributions, but that the ratios of the reactive to unreactive isomers depend on the cluster composition. Plotted in Figure 9 is the percentage of unreactive clusters, determined from the ratio of the signal corresponding to $p = 0$ to all the signals, for each of the 13-mers produced from the $Co_{0.85}Mn_{0.15}$ rod.

At the high-pressure end of the nitrogen uptake plots in Figures 6−8, $\bar{p}$ often reaches a particular value and remains constant over a considerable pressure range. This value corresponds to the maximum number of nitrogen molecules that can

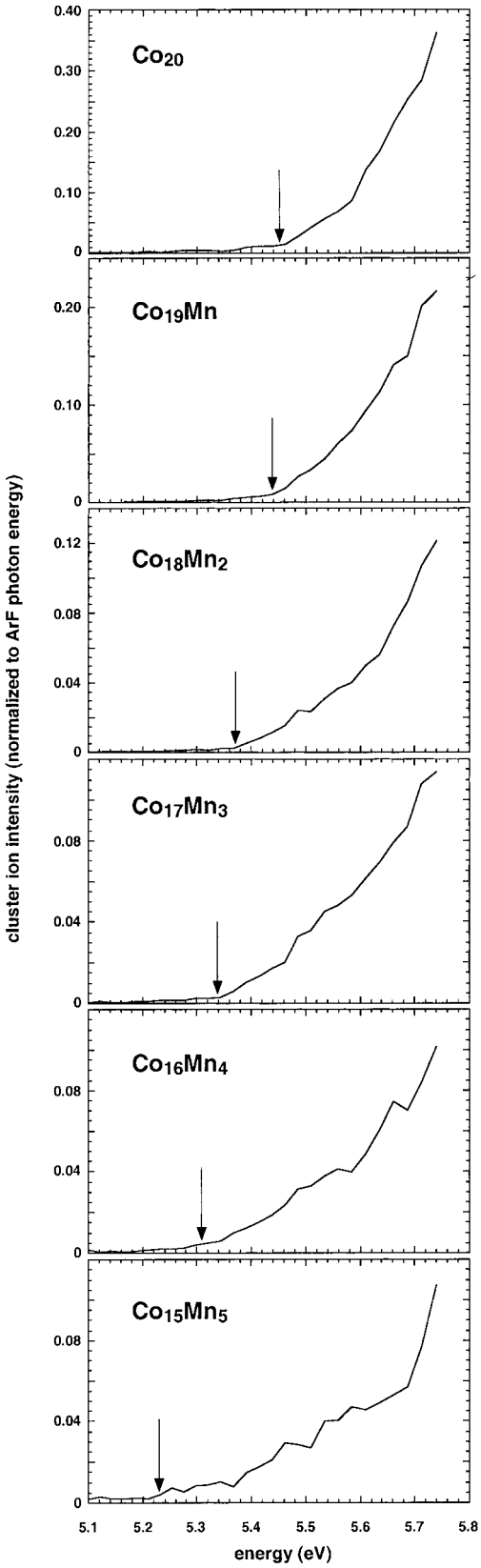

Figure 3. Photoionization efficiency spectra of Co_nMn_m, $n + m = 20$.

be adsorbed on the metal cluster (prior to condensation, which does not occur under these conditions). Certain trends in the dependence of this saturation value on cluster composition are evident in Figures 6−8, and we will discuss below saturation rules suggested by these data. In Figure 10, an uptake plot in

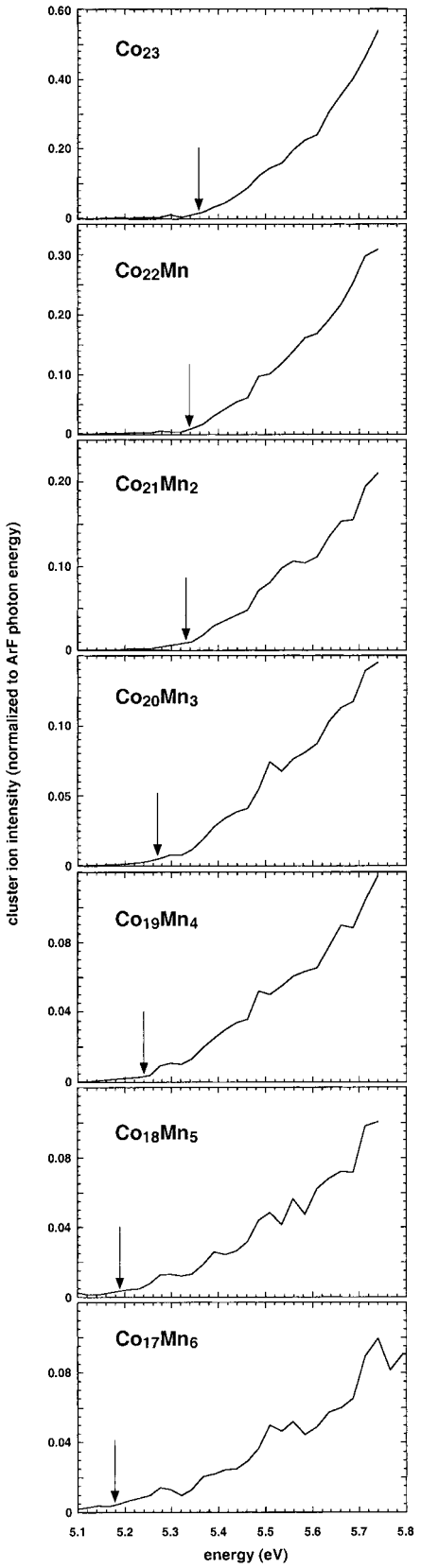

Figure 4. Photoionization efficiency spectra of Co_nMn_m, $n + m = 23$.

the high-pressure regime for 13-mers produced from the $Co_{0.5}Mn_{0.5}$ rod at −120 °C is shown to demonstrate that the saturation trends observed in Figure 7 for cobalt-rich clusters also apply for manganese-rich clusters. As will be discussed, the saturation rules remain the same over a broad range of temperatures for the 13-mers (and other cluster sizes having structures of high symmetry), but they are somewhat dependent on temperature when the cluster has sites of low coordination.

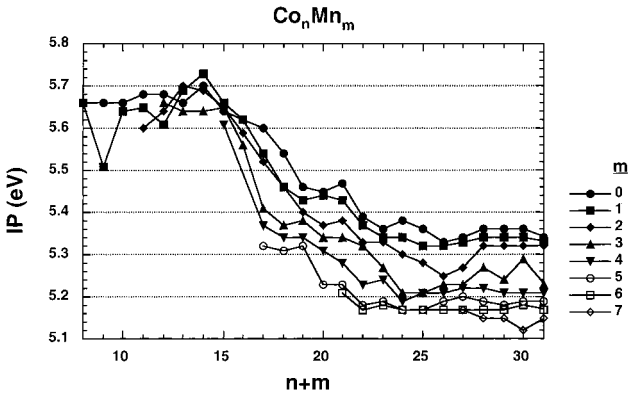

Figure 5. Vertical ionization potentials of Co_nMn_m. The uncertainty in assignment of IPs is estimated at ±0.05 eV.

TABLE 1: Vertical Ionization Potentials (in eV) for Co_nMn_m Clusters[a]

$n+m$	$m=0$	$m=1$	$m=2$	$m=3$	$m=4$	$m=5$	$m=6$	$m=7$
8	5.66	5.66						
9	5.66	5.51						
10	5.66	5.64						
11	5.68	5.65	5.60					
12	5.68	5.61	5.64	5.66				
13	5.66	5.71	5.70	5.64				
14	5.70	5.73	5.69	5.64				
15	5.64	5.66	5.65	5.65	5.61			
16	5.62	5.62	5.59	5.56				
17	5.60	5.54	5.52	5.41	5.37	5.32		
18	5.54	5.46	5.46	5.37	5.34	5.31		
19	5.46	5.43	5.40	5.38	5.34	5.32		
20	5.45	5.44	5.37	5.34	5.31	5.23		
21	5.47	5.43	5.38	5.34	5.28	5.23	5.21	
22	5.39	5.37	5.33	5.32	5.23	5.18	5.17	
23	5.36	5.34	5.33	5.27	5.24	5.19	5.18	
24	5.38	5.34	5.30	5.21	5.19	5.17	5.17	
25	5.36	5.32	5.28	5.21	5.21	5.17	5.17	
26	5.33	5.32	5.25	5.23	5.21	5.19	5.17	
27	5.34	5.33	5.27	5.23	5.22	5.20	5.17	5.17
28	5.36	5.34	5.32	5.27	5.22	5.19	5.17	5.15
29	5.36	5.34	5.32	5.24	5.21	5.18	5.17	5.15
30	5.36	5.34	5.32	5.29	5.21	5.19	5.18	5.12
31	5.34	5.33	5.32	5.23	5.21	5.19	5.17	5.15

[a] The estimated uncertainty of the assignments is ±0.05 eV.

4. Discussion

Ionization Potential vs Reactivity. One common feature of the PIE spectra displayed in Figures 2−4 is that as the amount of Mn in the Co_nMn_m clusters increases, the post-threshold increase in the relative photoionization cross section becomes less steep. (This is particularly clear in Figures 3 and 4. Note the differing *y*-axis scales. Recall that the PIE spectra are normalized to unity at 6.42 eV.) These differences in the shapes of the PIE spectra may be solely intrinsic, reflecting a fundamentally different distribution of electronic states in the Co_{n+m} versus Co_nMn_m cluster ions, or they may also reflect the existence of multiple isomers of Co_nMn_m having different IPs.[24]

There are two general trends in the IPs shown in Figure 5 and tabulated in Table 1: (1) for clusters containing more than 14 atoms, the IPs decrease rapidly as the cluster size increases, as for homonuclear transition metal clusters previously investigated; (2) for a given cluster size $n + m$, as the number of manganese atoms increases, the IP decreases. This latter result

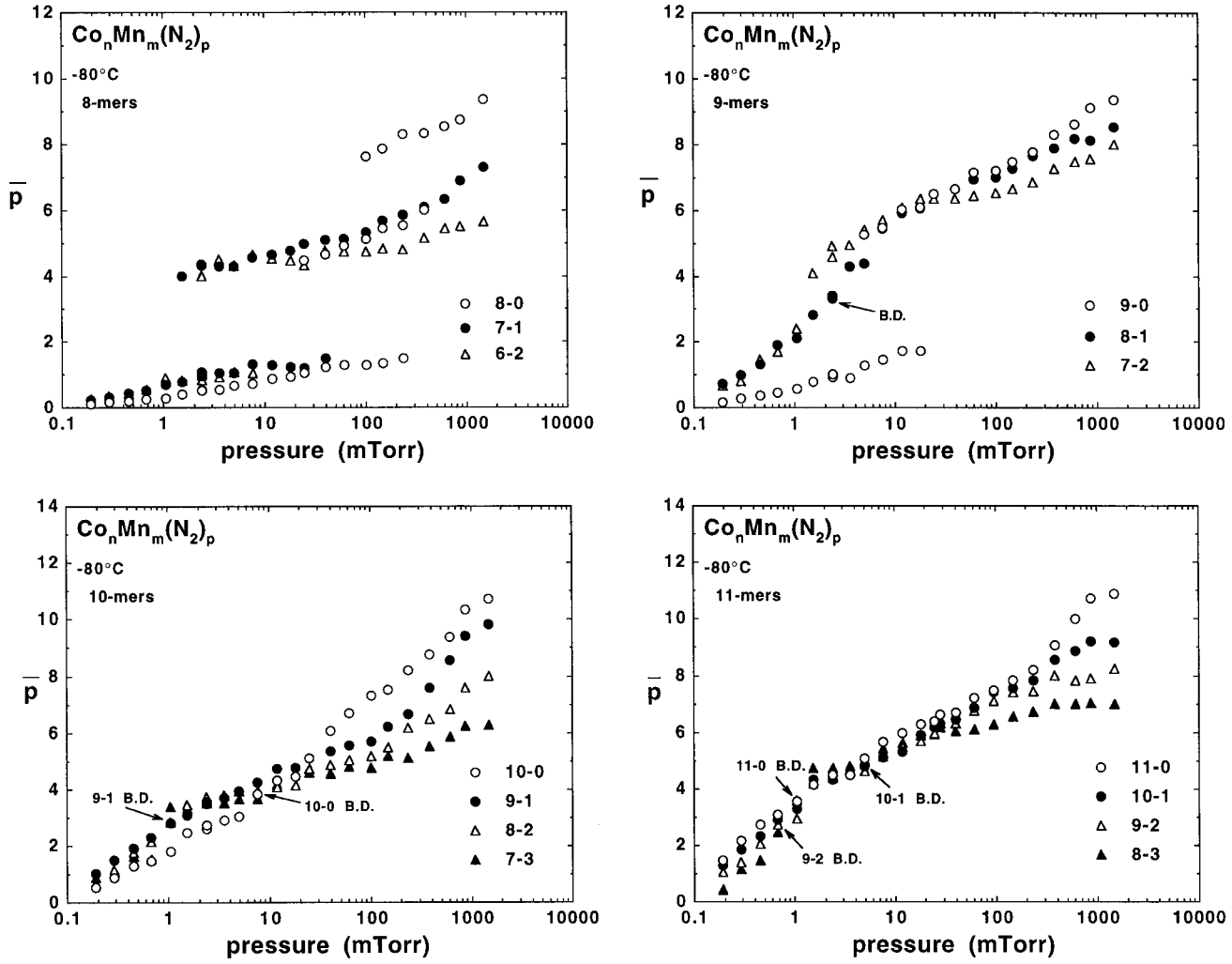

Figure 6. Nitrogen uptake plots for Co_nMn_m, $n + m = 8-11$. The temperature of the flow tube reactor is −80 °C. B.D. labels points that are averages over (unresolved) bimodal distributions in p.

is also to be expected because the IPs of manganese clusters[25] are smaller than those of the corresponding cobalt clusters.[23]

For facile association reactions of molecules with metal clusters, including the nondissociative adsorption of N_2, the most noticeable variations in reactivity with cluster size are observed under equilibrium conditions and correlate with variations in the atomic arrangement as determined by their geometries.[14,21,26] Such correlations form the basis for metal cluster structure investigation by the chemical probe method, as exemplified in this study. As expected for a facile reaction, there is no obvious correlation between the initial reactivity toward N_2 (i.e., at low coverage) and IP—a measure of cluster global electronic structure. In contrast, for activated reactions such as the dissociative chemisorption of H_2 and N_2 on metal clusters, the reaction rates (rather than equilibria) are more noticeably dependent on cluster size, and these rates have been found in some cases to correlate with global variations in the electronic structure of the metal cluster. In particular, for activated dissociative chemisorption of H_2 on Nb_n[27] and (to a lesser extent) on Fe_n,[28] an inverse dependence of reactivity with cluster IP has been observed, with local IP maxima corresponding to reactivity minima and vice versa. A simple model based on these observations postulates that electron transfer from the clusters' highest occupied molecular orbital (HOMO) to H_2 antibonding levels comprises the barrier for these activated reactions and that to first order, cluster IPs provide a measure of the barrier height.[29,30]

Pure cobalt clusters, while displaying the size variation in reactivity toward H_2 typical of other transition metal clusters,[15,31] do not exhibit any obvious IP−reactivity correlation.[23] The situation appears to be no different in mixed cobalt−manganese clusters. The IP measurements presented here for Co_nMn_m show that successive manganese atom substitution within cobalt clusters leads to lower IPs, yet Nonose et al. found that Mn-for-Co substitution within cobalt clusters did not appreciably affect their reactivity: $Co_{n-m}Mn_m$ clusters were determined to be approximately as reactive toward H_2 as the corresponding Co_n.[32] In a study of Co_nNa_m clusters by Hoshino et al.[33] it was found that sodium adatoms lowered the IPs of the cobalt clusters significantly but at the same time actually *lowered* their reactivities toward hydrogen. Extending this argument to the limiting case, we note that pure manganese clusters[25] possess significantly lower IPs than cobalt clusters[23] having the same number of atoms, yet are completely unreactive toward hydrogen below Mn_{16}.[34] Taken together, the available data indicate that the IP versus H_2 reactivity behavior of neither Co_n nor Co_nMn_m can be rationalized by simple electron-transfer arguments. These results tend to corroborate H_2 reactivity[7] versus IP[10] comparisons in other bimetallic cluster systems, where little or no relationship is observed. Given these observations, it is perhaps not surprising that little IP−reactivity correlation is found for the nondissociative adsorption of N_2 on Co_nMn_m clusters.

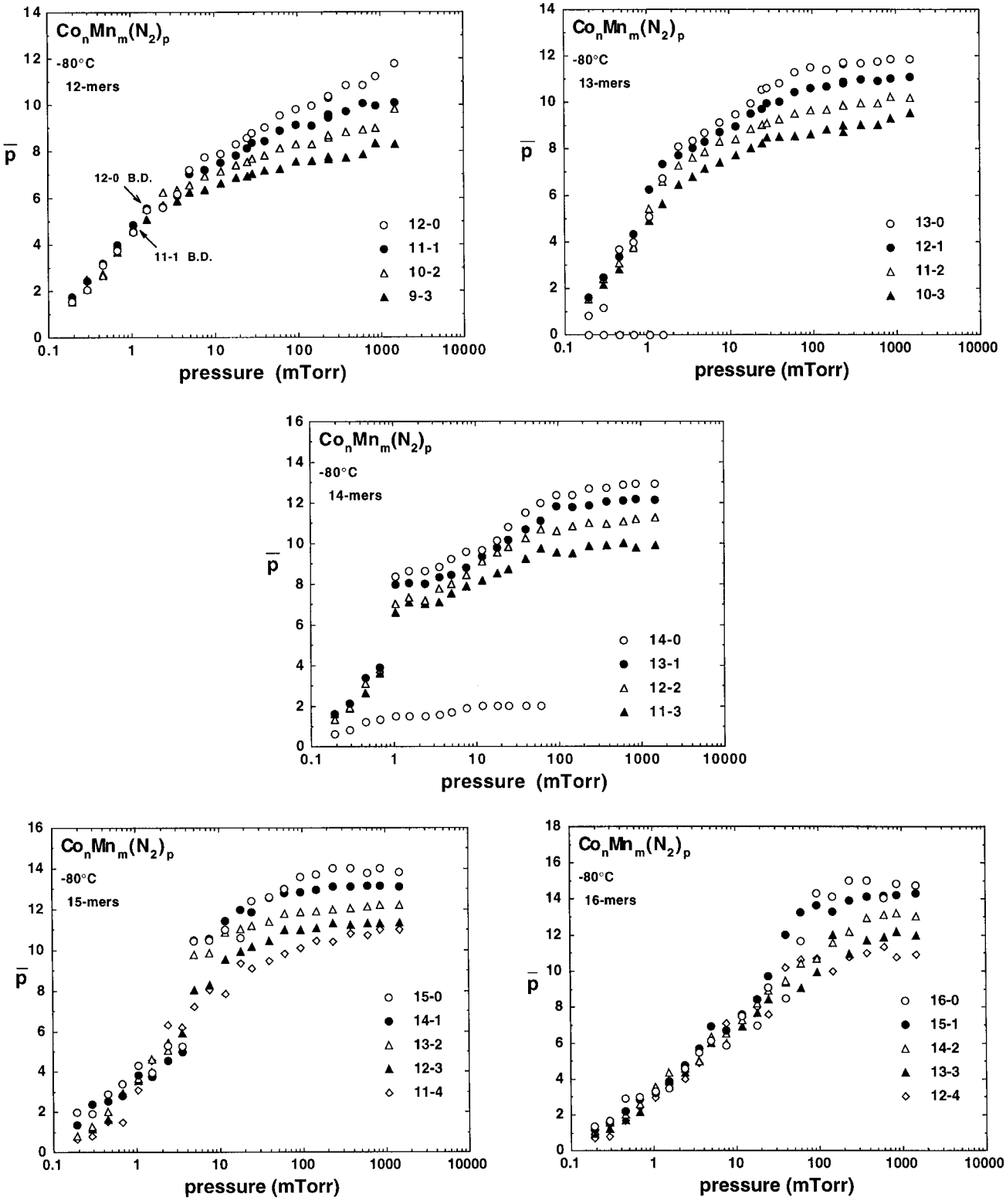

Figure 7. Nitrogen uptake plots for Co_nMn_m, $n + m = 12-16$.

Geometric Structures. Many of the uptake plots in Figures 6−8 show features that have been seen in other studies of nitrogen reactions with transition metal clusters.[21] At low nitrogen pressures, where adsorption kinetics dominate the extent of adsorption, the rise in $\bar{p}$ is rapid. Once the nitrogen pressure is sufficient for equilibrium adsorption, the increase in $\bar{p}$ tapers off. In cases where the uptake can be followed to even higher pressures, the value of $\bar{p}$ may become constant, indicating the cluster has become saturated with nitrogen molecules. Such saturation is seen in many of the uptake plots of Figures 6−8. In some cases (such as the 18-, 19-, and 20-mers) mass spectral congestion prevented following the uptake to high enough nitrogen pressures to observe saturation.

For a few of the clusters, (notably the 13-mers) $\bar{p}$ values at low nitrogen pressures are lower for the pure cobalt clusters than for the bimetallic ones. This raises the question of whether manganese increases the propensity of N_2 to bind to a cluster. Uptake measurements of N_2 on monometallic Co_n[14] and Mn_m[35]

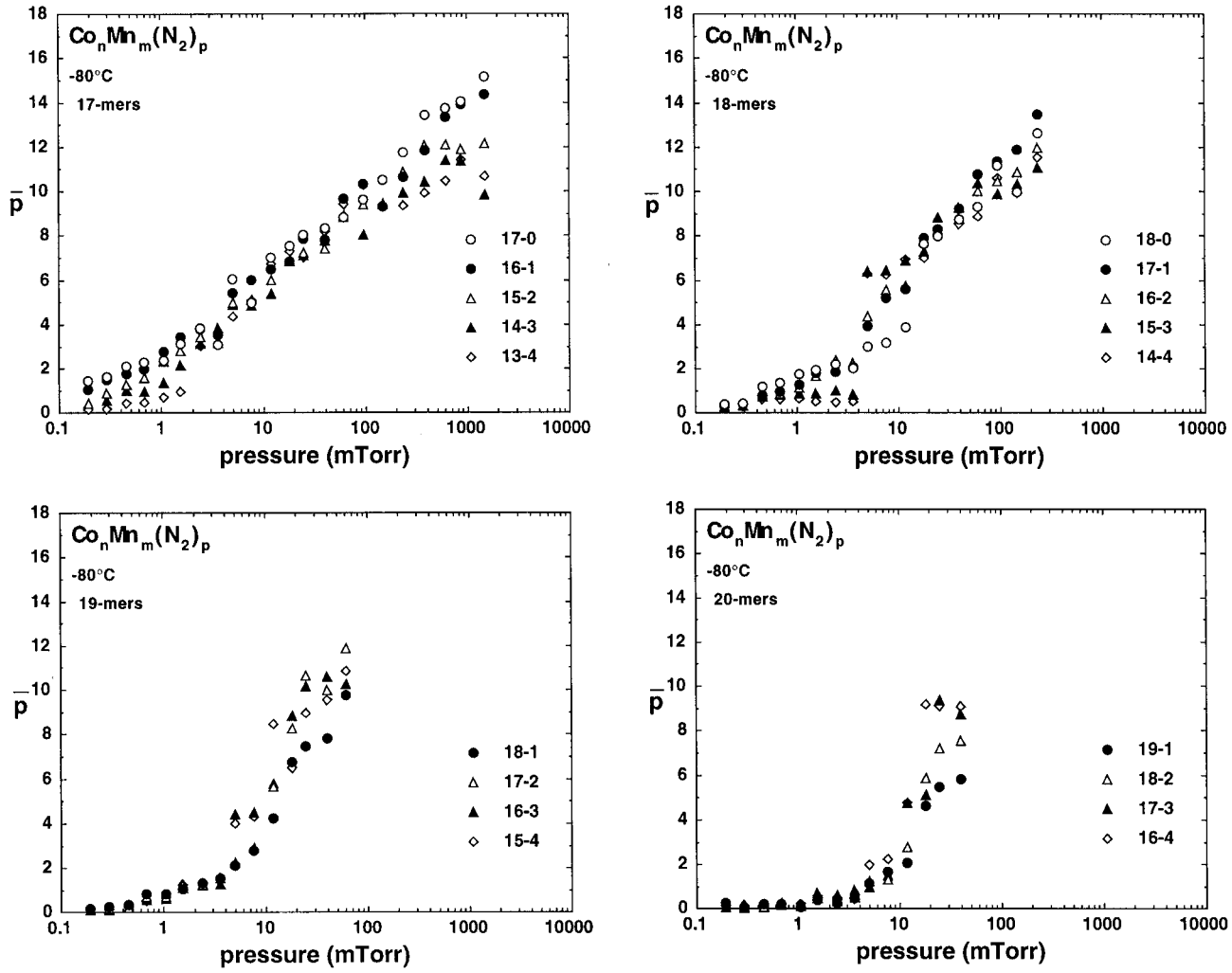

Figure 8. Nitrogen uptake plots for Co_nMn_m, $n + m = 17-20$.

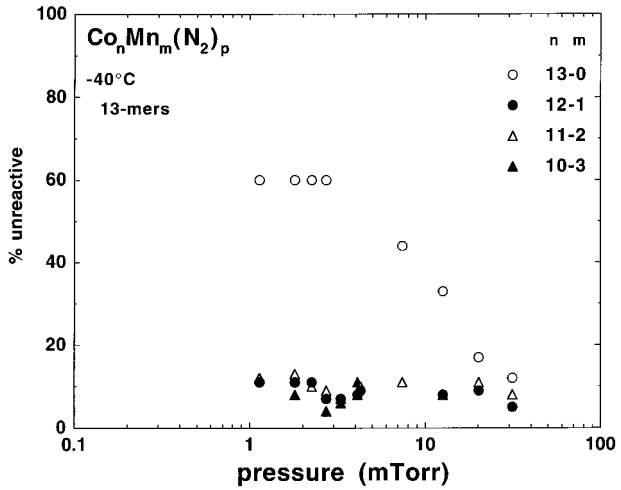

Figure 9. Percentage of Co_nMn_m, $n + m = 13$, that are unreactive as a function of pressure (see text). The temperature of the flow tube reactor is −40 °C.

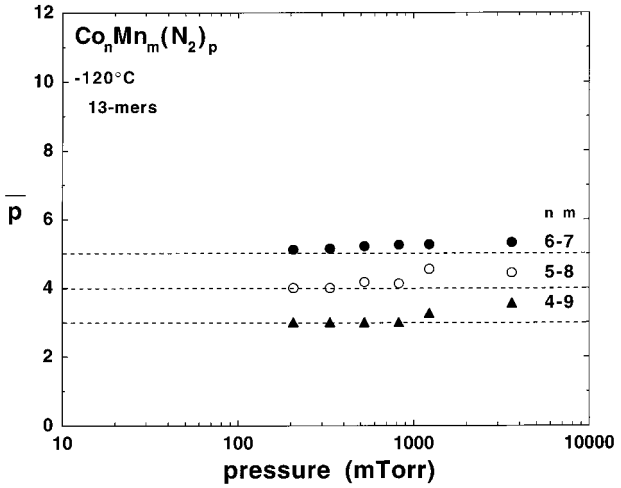

Figure 10. Nitrogen uptake plots for Co_nMn_m, $n + m = 13$. The temperature of the flow tube reactor is −120 °C.

demonstrate that cobalt clusters take up nitrogen molecules much more readily than do manganese clusters. (For example, a comparable coverage on Mn_{13} requires approximately 500 times greater N_2 pressure than for Co_{13}.) This suggests that nitrogen molecules bind preferentially to cobalt atoms in Co_nMn_m clusters. Hence, if Mn atoms increase the likelihood of N_2 binding to Co_nMn_m, they play a peripheral role, essentially "activating" the Co atoms to bind nitrogen molecules. However, another possibility is that manganese affects the cluster structure, which, in turn, affects the adsorption probability of N_2. This was illustrated in Figure 9, which demonstrates that manganese converts Co_{13} to a more reactive isomer. Previous studies[14] of the reactions of Co_n with N_2 showed that the lowest-energy isomer of Co_{13} is converted to a more reactive icosahedral structure, higher in energy for bare Co_{13}, upon adsorption of

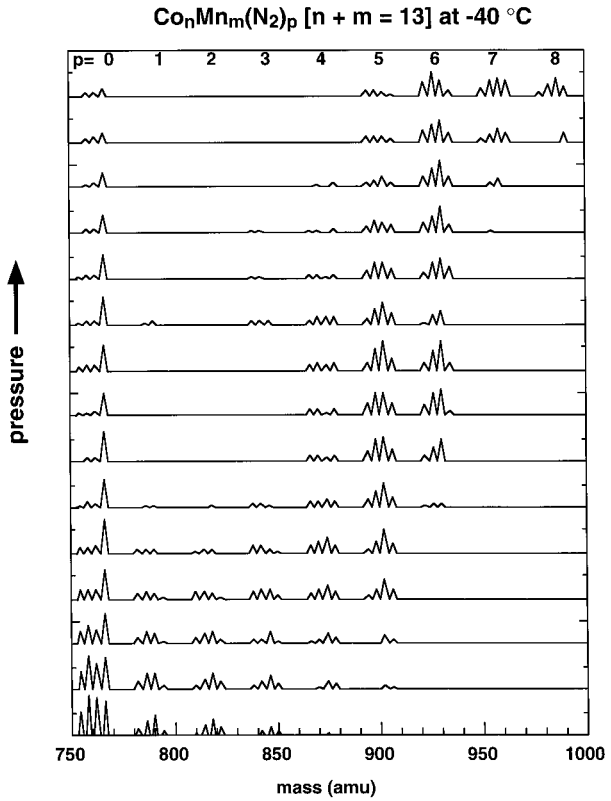

Figure 11. Time-of-flight mass spectrum of $Co_nMn_m(N_2)_p$, $n + m = 13$, produced using various pressures of N_2. The temperature of the flow tube reactor is −40 °C. The noise is filtered out of the spectrum to make viewing easier, but the peak positions and intensities are unaltered. Note that Co_{13} is less reactive toward N_2 than the Mn-substituted 13-mers, as evidenced by the persistence of the Co_{13} peak (the rightmost peak of the group of peaks for $p = 0$) with increasing N_2 pressure.

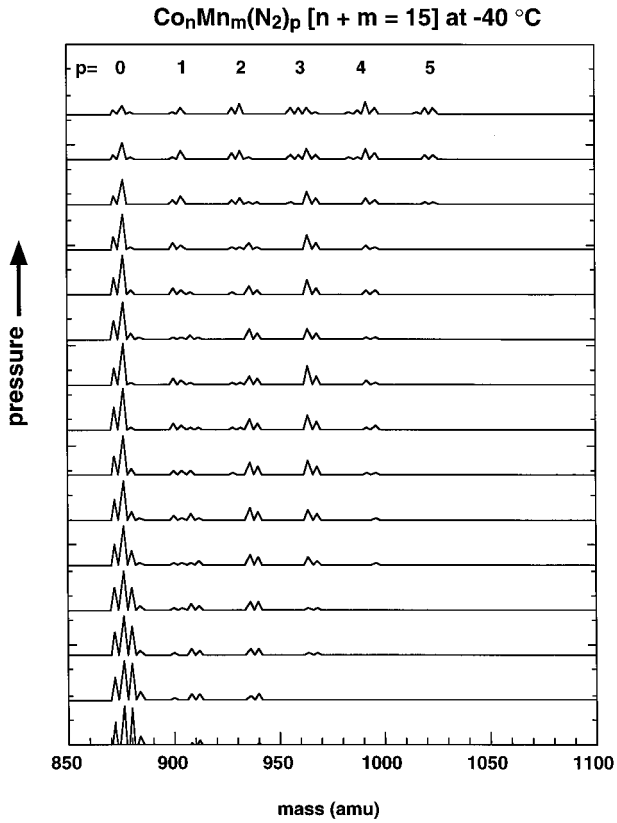

Figure 12. TOF mass spectrum of $Co_nMn_m(N_2)_p$ as in Figure 11, but for $n + m = 15$. Note that here the peaks corresponding to $Co_{12}Mn_3$ and $Co_{13}Mn_2$ (the leftmost pair of the group of peaks for $p = 0$) disappear more slowly with increasing N_2 pressure than those corresponding to $Co_{14}Mn$ and Co_{15}, indicating that $Co_{12}Mn_3$ and $Co_{13}Mn_2$ are less reactive than $Co_{14}Mn$ and Co_{15} toward N_2.

N_2. Thus, it appears that manganese can likewise bring about the same or a similar structural change for Co_{13}. This is to be contrasted with Co_{15}, where there is no evidence of structural rearrangement upon uptake of nitrogen and no apparent enhancement in nitrogen binding when manganese atoms are substituted for cobalt. These differences are illustrated in Figures 11 and 12, which show mass spectra at −40 °C and various N_2 pressures for $n + m = 13$ and $n + m = 15$. (The noise is filtered out of the spectra to make viewing easier, but the peak positions and intensities are unaltered.) It is apparent that while Co_{13} adsorbs nitrogen less readily than the bimetallic 13-mers, Co_{15} is more reactive toward N_2 adsorption than $Co_{13}Mn_2$ and $Co_{12}Mn_3$, for instance. This supports the hypothesis that manganese atoms do not inherently promote adsorption of N_2 onto a Co_nMn_m cluster, but they can shift the relative energies of close-lying isomers to favor a structure having more facile adsorption of nitrogen molecules.

We will now discuss the individual cluster sizes for which uptake plots are shown in Figures 6−8. Interpretations in terms of cluster structure are based on some assumed simple binding rules: nitrogen binds only to atop (single-atom) sites, preferentially to cobalt atoms, and the lower the metal−metal coordination of a binding site the higher its nitrogen adsorption binding energy.

4.1. 8-mers. The nitrogen uptake data for Co_8 is consistent with that previously reported.[14] Although not evident in the data in Figure 6, the mass spectra show that Co_8 takes up a maximum of two nitrogen molecules up to a pressure of ∼25 mTorr. Thereafter, more nitrogens are adsorbed, although the $Co_8(N_2)_3^+$ peak is weak or nonexistent throughout the entire pressure range. (That is, in the $Co_8(N_2)_p^+$ distribution, there is a jump from $Co_8(N_2)_2^+$ to $Co_8(N_2)_4^+$.) This suggests that the initial Co_8 isomer may have two sites that bind N_2 strongly and that uptake of more nitrogen is accompanied by a structural change. An initial structure consistent with this interpretation is the bicapped octahedron. (See ref 14 for further discussion.)

Both Co_7Mn and Co_6Mn_2 display the same initial behavior as Co_8 in their N_2 uptake, although the conversions to the more reactive isomers take place at lower nitrogen pressures. The low intensity of $Co_7Mn(N_2)_3^+$ and $Co_6Mn_2(N_2)_3^+$ at all N_2 pressures suggests that the initial isomers of Co_7Mn and Co_6Mn_2 are also bicapped octahedra, in which the capping atoms are cobalt. As for Co_8, little can be inferred from the uptake data about the structures of more highly nitrogen-covered species.

4.2. 9-mers. As in the earlier study, Co_9 takes up a maximum of three N_2 molecules at pressures below ∼4 mTorr. From 4 to 40 mTorr there is a bimodal distribution, with $Co_9(N_2)_4^+$ barely present in the mass spectrum. Two structures that are consistent with this behavior are the tricapped octahedron and the tricapped trigonal prism, both of which have three atoms that are low-coordinate (three-coordinate in the case of the tricapped octahedron and four-coordinate in the case of the tricapped trigonal prism) and therefore likely to bind N_2 more strongly than the remaining six cobalt atoms. In contrast, neither $Co_8Mn(N_2)_4^+$ nor $Co_7Mn_2(N_2)_4^+$ show anomalously low intensities at any pressure of nitrogen. Rather, low intensities are observed for $Co_8Mn(N_2)_5^+$ and $Co_7Mn_2(N_2)^+$, suggesting structures with four low-coordinate Co atoms and no low-coordinate Co atoms for Co_8Mn and Co_7Mn_2, respectively. The bicapped pentagonal

bipyramid structure does have four atoms that are four-coordinate, while the other five atoms have higher coordination, so this structure is a possibility for Co_8Mn, with the cobalt atoms occupying the low-coordinate positions. The absence of low-coordinate cobalt atoms in Co_7Mn_2 does not provide much structural information, aside from eliminating some possibilities having a highly symmetric core of eight atoms capped by a single cobalt atom. Of course, it is also possible that the manganese atoms occupy sites of low coordination.

4.3. 10-mers. For both Co_{10} and Co_9Mn, the intensities of the one-N_2 mass peaks are low at all pressures. As for Co_7Mn_2, it is difficult to draw structural inferences from such observations. On the other hand, for Co_8Mn_2 and Co_7Mn_3, the peaks corresponding to addition of four N_2 are barely observed at any pressure. An icosahedral-based tricapped pentagonal bipyramid structure for these clusters is consistent with the observations because it has three four-coordinate sites and seven higher-coordinate sites. The earlier study[14] indicated that Co_{10} undergoes several structural changes with increasing nitrogen coverage but that the final structure is the tricapped pentagonal bipyramid. If the bimetallic 10-mers in fact have this structure for all coverages, then this represents the first case in which substitution of manganese atoms into a cobalt cluster stabilizes an icosahedral structure. As discussed below, this effect continues for larger clusters.

The uptake data for the 10-mers show the first clear example of an apparent saturation rule: Co_nMn_m saturates with $n - 1$ nitrogen molecules. This rule also applies for the clusters (Co_8Mn_2, Co_7Mn_3, Co_6Mn_4, Co_5Mn_5, Co_4Mn_6, and Co_3Mn_7) produced from the $Co_{0.5}Mn_{0.5}$ rod. The interpretation of this rule is given below.

4.4. 11-mers. In the earlier study[14] it was argued that Co_{11} undergoes several structural changes with increasing nitrogen coverage and eventually adopts a structure consistent with a 13-atom icosahedron minus two adjacent surface atoms. $Co_{10}Mn$, Co_9Mn_2, and Co_8Mn_3 do not show any obvious evidence for structural changes at lower pressures, and all saturate with $n - 1$ nitrogen molecules at −80 °C. The $n - 1$ saturation level is also seen for 11-mers containing more manganese atoms (Co_7Mn_4, Co_6Mn_5, Co_5Mn_6, Co_4Mn_7, and Co_3Mn_8) produced from the $Co_{0.5}Mn_{0.5}$ rod. Such saturation is also consistent with an icosahedral 13-mer minus two adjacent atoms, providing the 10-coordinate "inside" atom is cobalt and that each of the surface cobalt atoms binds one N_2 molecule.[36] It seems likely that the central atom is cobalt, since the binding energy of Co_2 is 0.95 ± 0.30 eV,[37] much higher than the 0.44 ± 0.30 eV binding energy of Mn_2,[38] and the cohesive energy of cobalt, 4.29 eV, is larger than that of manganese, 2.92 eV.[39] In general, we expect cobalt atoms to occupy sites of high metal−metal coordination and manganese atoms to occupy low coordination sites.

4.5. 12-mers to 15-mers. At −80 °C, Co_nMn_m clusters of all compositions in this size range saturate with $n - 1$ nitrogen molecules. As discussed above for Co_{11}, the $n - 1$ saturation level is strongly suggestive of structures in which each external cobalt atom binds one N_2, while the external manganese atom(s) and the internal cobalt atom bind none. Structures based on the 13-atom icosahedron plus or minus surface atoms are consistent with these saturation values.

For the 12-, 13-, and 14-mers, discontinuities in the mass spectra and plateaus in the uptake plots suggest that clusters with fewer manganese atoms tend to show structural changes with increasing nitrogen coverage, while clusters with more manganese atoms are initially icosahedral and remain so as they take up N_2. For the 15-mers, as for Co_{15},[14] there is no evidence of a structural rearrangement for any composition. In this case the structure of all clusters is presumably a bicapped icosahedron.

At lower temperatures, such as −120 and −160 °C, Ho et al.[14] found that low-coordinate atoms on pure cobalt clusters in this size range will bind two nitrogen molecules, but this is not the case at −80 °C. In fact, we find that at −120 °C the 14-mers (compositions ranging from $Co_{13}Mn$ through Co_6Mn_8) adsorb a maximum of n N_2 and the 15-mers (compositions ranging from $Co_{14}Mn$ through Co_9Mn_6) adsorb a maximum of $n + 1$ N_2. Both these values are consistent with icosahedral structures in which the one (for $n + m = 14$) or two (for $n + m = 15$) low-coordinate cobalt atoms adsorb two nitrogen molecules.

4.6. 16-mers. Clusters ranging from Co_{16} through $Co_{12}Mn_4$ (the only ones investigated) saturate with $n - 1$ N_2 at −80 °C. At −40 °C the saturation level drops to $n - 2$. For the tricapped icosahedron formed with adjacent capping atoms (which maximizes their coordination) there is a surface atom that is nine-coordinate and will only bind nitrogen weakly. It is quite plausible that the binding energy for this atom is low enough that adsorption will not occur at −40 °C but will at −80 °C. In any case, the saturation levels are consistent with cobalt atoms occupying the highest coordination sites, as for the smaller clusters. Attempts to determine uptake patterns at temperatures lower than −80 °C for clusters larger than 15 atoms were made difficult by congested mass spectra, owing to the relative unreactivity of some of the larger clusters.

4.7. 17-mers to 19-mers. Clusters rich in cobalt in this size range are quite unreactive toward nitrogen, and saturation cannot be achieved even at −80 °C. Manganese-rich clusters, having fewer nitrogen binding sites, can be saturated, and at −40 °C the clusters produced from the $Co_{0.5}Mn_{0.5}$ target ($Co_{10}Mn_7$ through Co_7Mn_{10}, $Co_{12}Mn_6$ through Co_8Mn_{10}, and $Co_{12}Mn_7$ through Co_8Mn_{11}) all saturate with $n - 2$ N_2 molecules. This is consistent with additional capping of the 13-atom icosahedron until a double icosahedral structure results for the 19-mers. In this structure, there are two internal 12-coordinate atoms (presumably cobalt) that do not bind N_2 and 17 external atoms that, when cobalt, will each bind a single N_2 (12 six-coordinate atoms at either end of the cluster and 5 eight-coordinate atoms around the waist of the cluster). The observation that clusters richer in cobalt cannot be saturated with nitrogen is analogous to what has been reported for pure cobalt clusters: the N_2 adsorption energy drops sharply in the vicinity of $n = 19$ and 20.[15]

4.8. 20-mers to 23-mers. Whereas the 19-mers produced from the $Co_{0.5}Mn_{0.5}$ target saturate with $n - 2$ nitrogen molecules at −40 °C, the 20-mers at the same temperature bind a maximum of only $n - 4$ nitrogen molecules. The addition of a single atom at a 4-fold site around the waist of the double icosahedron causes two of the eight-coordinate atoms to become nine-coordinate. These atoms apparently do not bind N_2, and the added four-coordinate atom binds only a single nitrogen molecule at −40 °C. The saturation level changes to $n - 5$ N_2 at $n + m = 21$. This is consistent with the addition of another atom around the waist of the double icosahedron, causing one of the eight-coordinate atoms in the 20-mers (i.e., one of the waist atoms for which the coordination was not altered upon adding the 20th atom) to become nine-coordinate, and thereby nonreactive toward N_2 at −40 °C, and one of the nine-coordinate atoms to become 10-coordinate. The saturation level remains at $n - 5$ for the 22-mers and the 23-mers, consistent with further icosahedral growth. The polyicosahedral 23-atom cluster, which

can be viewed as three interpenetrating double icosahedra,[26] has 12 six-coordinate atoms and 6 eight-coordinate atoms, each of which bind a single N_2 at −40 °C, as well as 2 nine-coordinate atoms and 3 12-coordinate atoms, which bind no nitrogen molecules.

5. Conclusions

Using the reaction with N_2 as a chemical probe of bimetallic Co_nMn_m clusters, we have found that nitrogen preferentially binds to cobalt atoms, and from the saturation levels some insight into cluster structure can be provided. Small clusters composed of the two metals tend to follow an icosahedral growth sequence, in contrast to pure cobalt clusters, which adopt close-packed structures. No direct correlation between the IPs of Co_nMn_m and their reactivities with N_2 is observed.

Acknowledgment. We thank Dr. Eric Parks for his insight and helpful comments on the manuscript and Mr. Ben Backes for his help in processing the uptake data. This work is supported by the U.S. Department of Energy, Office of Basic Energy Sciences, Division of Chemical Sciences, under Contract No. W-31-109-ENG-38.

References and Notes

(1) Rodriguez, J. A. *Surf. Sci. Rep.* **1996**, *24*, 223.
(2) Dietz, T. G.; Duncan, M. A.; Powers, D. E.; Smalley, R. E. *J. Chem. Phys.* **1981**, *74*, 6511.
(3) Rohlfing, E. A.; Cox, D. M.; Petkovic-Luton, R.; Kaldor, A. *J. Phys. Chem.* **1984**, *88*, 6227.
(4) Taylor, T. G.; Willey, K. F.; Bishop, M. B.; Duncan, M. A. *J. Phys. Chem.* **1990**, *94*, 8016.
(5) Andrews, M. P.; O'Brien, S. C. *J. Phys. Chem.* **1992**, *96*, 8233.
(6) Nonose, S.; Sone, Y.; Onodera, K.; Sudo, S.; Kaya, K. *Chem. Phys. Lett.* **1989**, *164*, 427.
(7) Nonose, S.; Sone, Y.; Onodera, K.; Sudo, S.; Kaya, K. *J. Phys. Chem.* **1990**, *94*, 2744.
(8) Menezes, W. J. C.; Knickelbein, M. B. *Chem. Phys. Lett.* **1991**, *183*, 357.
(9) Menezes, W. J. C.; Knickelbein, M. B. *Z. Phys. D* **1993**, *26*, 322.
(10) Hoshino, K.; Naganuma, T.; Watanabe, K.; Konishi, Y.; Nakajima, A.; Kaya, K. *Chem. Phys. Lett.* **1995**, *239*, 369.
(11) Sone, Y.; Hoshino, K.; Naganuma, T.; Nakajima, A.; Kaya, K. *J. Phys. Chem.* **1991**, *95*, 6830.
(12) Klabunde, K. J.; Imizu, Y. *J. Am. Chem. Soc.* **1984**, *106*, 2721.
(13) Roberts, M. W.; McKee, C. S. *Chemistry of the Metal−Gas Interface*; Clarendon: Oxford, 1978.
(14) Ho, J.; Parks, E. K.; Zhu, L.; Riley, S. J. *Chem. Phys.* **1995**, *201*, 245.
(15) Morse, M. D.; Geusic, M. E.; Heath, J. R.; Smalley, R. E. *J. Chem. Phys.* **1985**, *83*, 2293.
(16) Parks, E. K.; Liu, K.; Richtsmeier, S. C.; Pobo, L. G.; Riley, S. J. *J. Chem. Phys.* **1985**, *82*, 5470.
(17) Mitchell, S. A.; Lian, L.; Rayner, D. M.; Hackett, P. A. *J. Chem. Phys.* **1995**, *103*, 5539.
(18) Mitchell, S. A.; Rayner, D. M.; Bartlett, T.; Hackett, P. A. *J. Chem. Phys.* **1996**, *104*, 4012.
(19) Knickelbein, M. B.; Yang, S.; Riley, S. J. *J. Chem. Phys.* **1990**, *93*, 94.
(20) Koretsky, G. M.; Knickelbein, M. B. *Eur. Phys. J. D* **1998**, *2*, 273.
(21) Parks, E. K.; Zhu, L.; Ho, J.; Riley, S. J. *J. Chem. Phys.* **1994**, *100*, 7206.
(22) Knickelbein, M. B.; Yang, S. *J. Chem. Phys.* **1990**, *93*, 5760.
(23) Yang, S.; Knickelbein, M. B. *J. Chem. Phys.* **1990**, *93*, 1533.
(24) Knickelbein, M. B.; Yang, S. *J. Chem. Phys.* **1990**, *93*, 1476.
(25) Koretsky, G. M.; Knickelbein, M. B. *J. Chem. Phys.* **1997**, *106*, 9810.
(26) Parks, E. K.; Zhu, L.; Ho, J.; Riley, S. J. *J. Chem. Phys.* **1995**, *102*, 7377.
(27) Whetten, R. L.; Zakin, M. R.; Cox, D. M.; Trevor, D. J.; Kaldor, A. *J. Chem. Phys.* **1986**, *85*, 1697.
(28) Whetten, R. L.; Cox, D. M.; Trevor, D. J.; Kaldor, A. *Phys. Rev. Lett.* **1985**, *54*, 1494.
(29) Conceição, J.; Laaksonen, R. T.; Wang, L.-S.; Guo, T.; Nordlander, P.; Smalley, R. E. *Phys. Rev. B* **1995**, *51*, 4668.
(30) Bérces, A.; Hackett, P. A.; Lian, L.; Mitchell, S. A.; Rayner, D. M. *J. Chem. Phys.* **1998**, *108*, 5476.
(31) Ho, J.; Zhu, L.; Parks, E. K.; Riley, S. J. *J. Chem. Phys.* **1993**, *99*, 140.
(32) Nonose, S.; Sone, Y.; Kaya, K. *Z. Phys. D* **1991**, *19*, 357.
(33) Hoshino, K.; Naganuma, T.; Yamada, Y.; Watanabe, K.; Nakajima, A.; Kaya, K. *J. Chem. Phys.* **1992**, *97*, 3803.
(34) Parks, E. K.; Nieman, G. C.; Riley, S. J. *J. Chem. Phys.* **1996**, *104*, 3531.
(35) Unpublished results from this laboratory.
(36) It should be noted that saturation with $n - 1$ N_2 is also consistent with other structures containing one internal atom, such as face-centered cubic (fcc) and hexagonal close-packed (hcp). However, it is argued in ref 14 that Co_{13} saturated with N_2 is icosahedral. Furthermore, saturation values for Co_nMn_m with larger $m + n$ are consistent with icosahedral packing but not fcc or hcp.
(37) Shim, I.; Gingerich, K. A. *J. Chem. Phys.* **1983**, *78*, 5693.
(38) Morse, M. D. *Chem. Rev.* **1986**, *86*, 1049.
(39) Kittel, C. *Introduction to Solid State Physics*; 6th ed.; Wiley: New York, 1986.